Undergraduate Journal of Experimental Microbiology and Immunology (UJEMI) Vol. 28:1-14

Towards an *in vitro* model of NLRP3 inflammasome activation via refining measures of IL-1β secretion and inflammasome assembly

Betty Yao, Iris Zhou, Sahar Malekighomi, Jong Yoon Joo

Department of Microbiology and Immunology, University of British Columbia, Vancouver, British Columbia, Canada

SUMMARY The formation of the (NOD)-like receptor protein 3 (NLRP3) inflammasome, an intracellular multiprotein oligomer, drives the secretion of pro-inflammatory cytokines such as IL-1β and IL-18 and inflammatory modes of cell death in response to microbial infection and cellular damage. As aberrant inflammasome function is implicated in a wide range of diseases, the proper characterization of its underlying mechanisms and regulation is key to understanding its potential as a therapeutic target. Here, we present an updated *in vitro* cell culture model of the NLRP3 inflammasome using lipopolysaccharide (LPS)-primed, nigericin-activated J774A.1 macrophages. Phase-contrast microscopy, Western blotting and ELISA were used to evaluate changes in cell morphology and mature IL-1β expression, respectively. Immunocytochemistry was used to detect apoptosis-associated speck-like protein containing a CARD (ASC) speck formation in nigericin-treated macrophages. While experimental approaches to mature IL-1β measurement require further development, we observed distinctive, irregular nigericin-induced morphological changes and the formation of ASC specks as likely indicators of NLRP3 inflammasome activation, making our cell culture model suitable for future research.

INTRODUCTION

The first line of host defense against pathogens is mediated by the innate immune system (1). In response to foreign and intrinsic stimuli, such as pathogen-associated molecular patterns (PAMPs) and damage-associated molecular patterns (DAMPs), leukocytes induce a variety of inflammatory responses leading to signaling pathways to activate further downstream effects (2). Inflammasomes are multi-protein complexes that play a vital role in regulating the innate immune system through inflammatory signaling (3). The nucleotide-binding oligomerization domain-like (NOD-like) receptor, pyrin domain-containing 3 (NLRP3) inflammasome is a critical component of the innate immune system expressed predominantly in macrophages. NLRP3, together with the adaptor protein apoptosis associated speck-like protein containing a CARD (caspase activation and recruitment domain) (ASC), forms a caspase-1 activating complex known as the NLRP3 inflammasome. It is responsible for detecting PAMPs and DAMPs such as nigericin and extracellular adenosine triphosphate (ATP), respectively (1). The assembly of the NLRP3 inflammasome leads to proteolytic activation of proinflammatory cytokines and caspases to drive further immune responses including the cleavage of pro-interleukin-1β (pro-IL-1β), pro-IL-18, and gasdermin D (GSDMD) into their active forms (1). IL-1β goes on to induce the expression of genes that control fever, vasodilation, and hypotension. Moreover, the activation of the NLRP3 inflammasome ultimately leads to inflammatory cell death through GSDMD-mediated pore formation, or pyroptosis (4). Aberrations in NLRP3 inflammasome function exists in a host of autoimmune and neurodegenerative diseases including Alzheimer's disease, atherosclerosis, diabetes, colitis (4), and cryopyrin-associated periodic syndromes (5, 6). Dysregulated inflammasome activity could have a crucial effect on the immune response. Therefore, regulation of inflammasome activity and therapeutic intervention is a promising area for clinical research.

Currently, a two-signal model has been proposed for NLRP3 inflammasome activation. The priming signal (signal 1) is provided by microbial components such as LPS or endogenous cytokines, leading to the activation of transcription factor nuclear factor kappa B

Published Online: September 2023

Citation: Yao, Zhou, Malekighomi, Joo. 2023. Towards an *in vitro* model of NLRP3 inflammasome activation via refining measures of IL-1β secretion and inflammasome assembly. UJEMI 28:1-14

Editor: Lauren Pugsley and Shruti Sandilya, University of British Columbia

Address correspondence to: https://jemi.microbiology.ubc.ca/

(NF-κB) and subsequent upregulation of NLRP3 and pro-IL-1β. NLRP3 is expressed at basal levels that are inadequate for initiating inflammasome activation under resting conditions and pro-IL-1β is not constitutively expressed in resting macrophages (3). Priming signals do not appear to affect the expression levels of ASC, pro-caspase-1, and pro-IL-18 (7). It is thought that the priming signal mainly plays a transcriptional role in NLRP3 inflammasome activation by up-regulating NLRP3 and pro-IL-1β. The NLRP3 inflammasome is then activated by a wide range of stimuli following this priming step (signal 2), including: ATP, particulate matter (8), pathogen-associated RNA (9), and nigericin, a K^+ ionophore derived from *Streptomyces hygroscopicus* (9, 10). The unifying factor of these activators is that they all induce cellular stress pathways. These pathways culminate in NLRP3 activation and inflammasome formation, but its mechanisms remain to be fully elucidated. K^+ efflux in particular is recognized as a common ionic event that occurs in cells treated with most NLRP3 inflammasome-activating stimuli. Cytosolic depletion of K^+ was found to mediate the maturation and secretion of IL-1β from macrophages in response to nigericin (9, 10).

Attempts to activate the NLRP3 inflammasome have proven challenging; past research groups have encountered numerous challenges developing a functional cell culture model to study the inflammasome, largely due to issues in obtaining the experimental readouts required to actually confirm that inflammasome activation is taking place (11–13). While these past studies were able to induce cell death via a priming signal (LPS) followed by an activation signal (ATP), they were unable to demonstrate that IL-1β was being processed from its pro- to mature, cleaved form in their cell culture models (11–13), thus rendering their attempts to develop a proper working model incomplete.

In this study, we aimed to optimize the specific *in vitro* cell culture and IL-1β quantification methods for the study of the NLRP3 inflammasome response in J774A.1 murine macrophages. We also aimed to visualize cellular morphology changes in response to LPS priming and nigericin activation through phase contrast microscopy. Following LPS priming, we hypothesized that subsequent activation with nigericin would induce NLRP3 inflammasome assembly and its downstream effects including caspase-1 mediated cleavage of pro-IL-1β into its cleaved mature IL-1β form and its secretion. We conducted Western blot analysis to detect the pro- and cleaved forms of IL-1β, and enzyme-linked immunosorbent assay (ELISA) to detect secreted IL-1β.

Finally, to resolve conflicting reports on the activation of the NLRP3 inflammasome, we used immunofluorescence microscopy to visualize ASC speck localization within the cell following inflammasome activation. Due to past difficulties in detecting mature IL-1β in both macrophage cell lysate and supernatant, we sought to have an alternative method to confirm NLRP3 inflammasome activation. While they primarily serve as an adaptor molecule key to the formation of the NLRP3 complex itself, ASC protein can also aggregate into specks (14). These ASC specks serve as a signal amplification mechanism for the main NLRP3 inflammasome, inducing stronger inflammatory responses through accelerating caspase-1 activation and subsequent IL-1β maturation (15, 16).

Here, we showed that LPS-primed, nigericin-activated J774A.1 murine macrophages upregulate the expression of pro-IL-1β and respond to nigericin treatment through morphological changes and vacuole formation. While cleaved IL-1β was not detected in our ELISA, we were able to visualize clear ASC speck formations which suggests NLRP3 inflammasome activation.

METHODS AND MATERIALS

Cell culture. J774A.1 mouse macrophages (Kronstad Lab, Michael Smith Laboratories, UBC) were cultured in complete media (DMEMc). Complete media was made from Dulbecco's Modified Eagle Medium (DMEM; Thermo Fisher Scientific, 11965118) supplemented with 10% fetal bovine serum (Thermo Fisher Scientific, A3160701) and 2 mM L-glutamine (Thermo Fisher Scientific, 25030-081). The cells were grown in an incubator with 5% CO2 at 37 °C. Every 2 or 3 days, the cells were sub-cultured by scraping for experimental or maintenance for a maximum of passage 20. For protein lysate and cell supernatant collection, cells were seeded in 6-well plates at a density of 300 000 cells/well, in a total volume of 2 mL. A 1 mg/mL stock solution of LPS (Sigma-Aldrich, L4391) was

diluted with DMEMc to make 500 ng/mL aliquots of LPS for priming the cells. Nigericin (Sigma Aldrich, N7143-5MG) was diluted in 100% methanol to make stock aliquots at 10 mg/mL. The nigericin aliquots were then diluted in DMEMc to make a 10 μM working solution for treating the cells. All stock solutions were stored at -20°C between experiments and equilibrated to room temperatures before use. The cells were treated with LPS (500 ng/ml) or 1x PBS (equal volume) for 4 hours, followed by stimulation with methanol (equal volume) or nigericin (10 μM) for 45 minutes and 2 hours.

Protein extraction and Pierce™ Bicinchoninic Acid (BCA) assay. Protein lysis buffer was prepared by dissolving 1 cOmplete ULTRA tablet protease inhibitor (Roche - Sigma 11697498001) in Triton X-100 lysis buffer (20 mM Tris, 137 mM NaCl, 10% glycerol, 2 mM EDTA, 1% Triton X-100). For cell lysis, a maximum of 100 μL of ice-cold lysis buffer was added to cell pellets prior to incubation on ice for 15 minutes. The sample was then centrifuged at 14 000 RPM for 10 minutes at 4°C. The supernatant was recovered, and protein concentration was measured using the BCA Protein Assay Kit (ThermoFisher, 23225) per manufacturer's instructions.

Cell culture supernatant preparation for protein analysis. Cell culture media collected from J774A.1 cells was centrifuged at 14 000 RPM for 5 minutes at 4°C. This supernatant was removed and stored at -20°C. Supernatant samples were concentrated using Ultra-15 Centrifugal Filter Units (MilliporeSigma™, UFC900308), per manufacturer's instructions. Final protein concentration was then measured using BCA Protein Assay Kit (ThermoFisher, 23225) according to manufacturer's instructions.

SDS-PAGE & Electrophoretic Transfer. Whole cell protein lysate and concentrated cell culture supernatant samples were diluted in Triton X-100 lysis buffer and 4x SDS-PAGE sample buffer, such that 20 μg of protein could be loaded per well. 4% acrylamide/bis stacking gel and 10% acrylamide/bis resolving gel were prepared according to the Mini-Protean Tetra Cell - Instruction manual (BioRad). Protein samples along with Spectra Multicolor Broad Range Protein Ladder (ThermoFisher, 26634) were run at 180V on SDS-PAGE gel for 60 min. A wet gel transfer was performed overnight at 30V and 4°C using a Hybond-P:PVDF (polyvinylidene difluoride) membrane (BioRad), transfer buffer (25 mM Tris-HCl pH 8.3, 192 mM glycine, 20% (v/v) methanol) (BioRad), and Trans-Blot® Electrophoretic Transfer Cell (BioRad, 1703946). Ponceau S dye confirmed equal loading. The membrane was stored in TBS-T at 4°C ahead of Western Blotting.

Western Blot. Membranes were blocked in 5% BSA+TBS-T (Tris-buffered saline with Tween-20) for 45 min. IL-1β was visualized through incubating the membrane 1:1000 mouse IL-1β/IL-1F2 Antibody (R&D Systems, Cat no. AF-401-NA) in 1% BSA-TBS-T for 90 minutes followed by 1:15 000 goat anti-mouse IgG-HRP conjugate (Invitrogen, Cat no. 31430) in 1% BSA+TBS-T for 45 minutes. HRP activity was detected by enhanced chemiluminescent (ECL) substrate (1:1 luminol: peroxide; ThermoFisher) and subsequent image acquisition via ChemiDoc MP Imager (BioRad). For re-probing, membranes were incubated protein-side up in 15 mL of stripping buffer (200 uM glycine, 3.4 uM SDS, 1% Tween-20, pH 2.2) for 20 minutes before re-blocking as previously described. To visualize β-actin, the membrane was incubated in 1:5000 monoclonal mouse anti-β-actin (Sigma Aldrich, A5316) diluted in 1% BSA+TBS-T for 90 minutes followed by 1:10000 monoclonal rabbit anti-goat secondary antibody (Jackson ImmunoResearch, AB_2339400) diluted in 1% BSA+TBS-T for 45 minutes. Detection of HRP activity and imaging was performed as previously described. All incubations were done at room temperature.

ELISA. Concentration of secreted IL-1β in cell culture supernatants were measured using the IL-1β Mouse ELISA kit (ThermoFisher, 88-7013-86) according to manufacturer's instructions. The absorbance measurements of recombinant IL-1β standards at 450 nm (y-axis) were plotted against their known concentration (x-axis).

Actin Labelling & Epi-fluorescence Imaging. J774A.1 mouse macrophage cells were seeded on glass coverslips in a 12-well plate at a density of 100 000 cells/well, and then incubated for 24 h at 37°C, 5% CO2. The cells were treated with LPS (500 ng/ml) or 1x PBS (control) for 4 h, followed by stimulation with methanol (control) or 10 µM nigericin for 45 minutes and 2 h.

Fixing solution was prepared by diluting Pierce™ 16% Formaldehyde (w/v), Methanol-free (Thermo Fisher, 28906) to a 4% working solution in 1x PBS. Cells were incubated in fixing solution for 15 minutes at room temperature. For storage, fixed cells were kept in 1x PBS at 4℃, protected from light. Fixed cells were then incubated in blocking solution (1x PBS+1% BSA) for 1 hour ahead of permeabilization in 0.25% Triton X-100 (Sigma, CAS#9002-93-1) solution prepared in 1x PBS+1% BSA for 10 minutes. Both blocking and permeabilization steps were carried out at room temperature. The F-actin cytoskeleton was labelled using 1.0% Alexa-Fluor™ 568 Phalloidin Fluorophore Conjugate (Invitrogen, A12380) diluted in 1x PBS+1% BSA for 40 min protected from light. Nuclear counterstaining was performed by incubating samples in 0.1% DAPI solution (1 mg/mL) (Thermofisher) diluted in 1xPBS+1%BSA for nuclei visualization. ProLong Gold Mounting Media (Thermofisher, Cat#: P10144) was added on a glass slide, then the coverslips were mounted on the glass slide and sealed using clear nail polish. Fluorescence images were captured by ZEISS Axioscope using the 100x objective.

ASC Speck Staining & Epi-fluorescence Imaging. J774A.1 mouse macrophage cells were seeded on glass coverslips in a 6 well plate at a density of 100,000 cells/well, and then incubated for 24 hours at 37°C, 5% CO2. The cells were treated with each condition. Subsequently, the cells were fixed in ice-cold methanol for 15 minutes on ice, and then stored in 1x PBS at 4℃. Fixed cells were then incubated in blocking solution (1x PBS+1% BSA) for 1 hour ahead of incubation for 1 hour in dark at room temperature with 1:150 ASC anti-mouse monoclonal antibody (Santa Cruz Biotechnology, Cat# sc-514414), wash with 1X PBS 3 times, followed by an incubation for 1 h in dark at room temperature with 1:2000 goat anti-mouse Alexa Fluor™ 568-phalloidin secondary antibody (Invitrogen, A11001) diluted in 1xPBS+1%BSA. Then, 3 minutes staining in dark with 0.1% DAPI solution (Thermofisher) diluted in 1xPBS+1%BSA for nuclei visualisation was performed. ProLong gold mounting media was added on a glass slide, then the coverslips were mounted on the glass slide and sealed using a nail polish. The fluorescence photomicrographs of the stained cells were observed and captured using the Zeiss Axioscope upright epi-fluoresnce microscope (100X objective lens magnification).

NucGreen Cell Assay. J774A.1 cells were seeded at a density of 100,000 cells/well in a 12-well plate and incubated overnight at 37°C, 5% CO2. The cells were treated with LPS (500 ng/ml) or

1xPBS (control) for 4 h, followed by stimulation with methanol (control) or 10 µM nigericin for 45 min and 2 h. NucGreen Dead 488 (ThermoFisher, Cat#R37109) stain was added as per manufacturer instructions to visualize cell viability using an inverted Zeiss Axioscope epi-fluorescence microscope equipped with a monochrome camera. All images were captured using the 40X objective lens.

ImageJ Densitometry Analysis and Cell Area Quantitative Analysis. Densitometry analysis for both ChemiDoc Western blot pro-IL-1β and β-actin images was performed using the ImageJ software. The pixel intensity of pro-IL-1β protein bands in Western blot were semi-quantified relative to the pixel intensity of β-actin bands in each lane on the membrane. Prism9 software was used to generate a graph, representing the relative pixel intensities for LPS or PBS treated samples stimulated with methanol or 10 µM nigericin for 45 minutes and 2 hours.

Epi-fluorescence images of macrophages stained with DAPI and Alexa Fluor 568-phalloidin were pseudo-coloured using ImageJ software. Cell area quantification, measurement of vacuole diameter and vacuole density within cells was performed using ImageJ. True image dimensions (i.e., number of pixels representing one µm of length) were set according to the micrograph's accompanying scale bar. The surface area of 30

representative cells per condition were then taken via the freehand selection tool. Vacuole diameter was measured by taking the elliptical selection tool to first measure the area of 30 representative vacuoles per condition, and then plugging it into the following equation to obtain vacuole diameter.

$$\sqrt{\frac{Vacuole\ area}{\pi}} = Vacuole \text{ diameter}$$

Vacuole density was obtained by first measuring the area of a macrophage and quantifying the total number of vacuoles within said cell. The total number of vacuoles was then divided by the total cell area. 10 representative cells per condition were used. All data was imported to RStudio software to generate graphs. A sample script is provided in a supplementary file.

Data and Statistical Analysis. Data wrangling, visualization, and statistical analysis were performed on RStudio via the Tidyverse package. All bar plots are expressed as mean ± SD.

RESULTS

LPS-primed J774A.1 macrophages develop distinctive, irregular cell morphological features with higher surface area and undergo vacuolization in response to nigericin. To establish and optimize our working model of the NLRP3 inflammasome activation, we first treated J774A.1 macrophages with LPS (500 ng/ml) as a priming signal or 1x PBS (as a control) for 4 hours, and then stimulated with a methanol-only control or 10 μM nigericin for either 45 minutes or 2 hours as an activating signal. Phase-contrast and epi-fluorescence microscopy were then used to assess optimal stimulation times for our model based on morphological observations (FIG. 1, Supplementary FIG 1). LPS-primed macrophages adopted elongated morphologies with pseudopodia formation, which are characteristic of pro-inflammatory macrophages (17) (FIG. 1A, third row). Conversely, macrophages treated with a vehicle control retain a rounded morphology, indicating a lack of macrophage activation (FIG. 1A, top). Exposure to nigericin following LPS priming induces unique changes distinct from the phenotypes seen in either control or LPS-only treatment, producing highly irregular morphologies with some vacuoles forming inside of the cell. While they become larger, they lose any semblance of cell polarity induced by prior LPS stimulation and begin to form high amounts of vacuoles, which are identifiable as white circular structures within the cell under phase-contrast microscopy (FIG. 1A) that vary from 0.2-3 μm in diameter. The macrophages also become more translucent; cell nuclei are now visible, while they had not been identifiable at all in our control and LPS-only treatment groups. 45 minutes following nigericin treatment, macrophages see a 4-fold increase in cell surface area with respect to the control and a 1.7-fold increase with respect to LPS-only treated macrophages. This dramatic increase in cell surface area appear to wane over time; after two hours of nigericin exposure, macrophages still bear irregular morphologies with a number becoming small and rounded as they appeared to have lifted off the cell culture plate surface and are now only have a surface area 3.1 times greater than the control, or 1.2 times greater than macrophages treated with LPS only.

In addition to noting changes in overall morphology and surface area, we also quantified fluctuations in vacuole diameter and quantity between macrophages treated with LPS alone and those subsequently activated with nigericin (FIG. 1C, D). Vacuole size appears to peak at about 45 minutes of nigericin exposure, with a median diameter of 1.5 μm, increasing from 0.8 μm in the LPS-only treatment group. The number of vacuoles within each cell also steadily increases upon nigericin activation; macrophages begin to upregulate vacuole formation within 45 minutes of exposure, and vacuole quantity continues to increase 2 hours following exposure. It should be noted that while the 2-hour nigericin condition bears the highest vacuole among all conditions, the median vacuole diameter shrinks to levels comparable to the LPS-only condition.

These morphological changes following nigericin stimulation in macrophages pretreated with LPS are completely distinct from the changes seen in our control groups and our cells treated with LPS only. Our cell culture model, therefore, appears to induce a unique response in the cell, showing promise that our approach could possibly be effective at activating the NLRP3 inflammasome. As this was still preliminary data, we then moved on to gather more data to support our hypothesis.

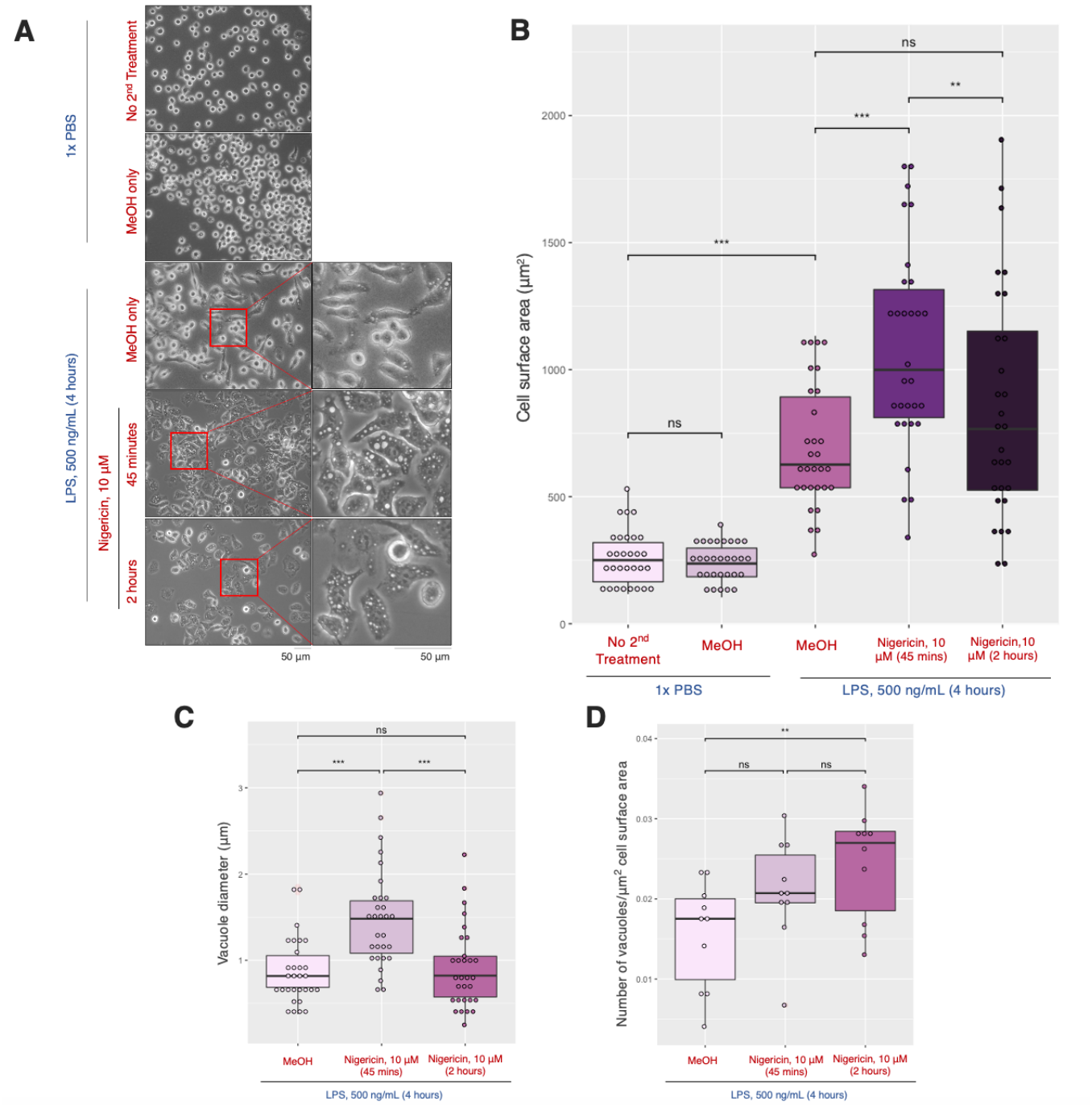

FIG. 1 LPS-primed J774A.1 murine macrophages are responsive to Nigericin stimulation. (A) Representative phase contrast images (40X) of J774A.1 cells following 4-hour LPS (500 ng/mL) priming for and nigericin (10 µM) stimulation for 45 minutes or 2 hours. PBS and ethanol serve as control. *Scale bar* 50 µm. (B) Quantification of median cell surface area respectively, in control versus treated macrophages. Number of cells analyzed per condition = 30. ANOVA and Tukey ***($p \leq 0.001$). (C) Quantification of vacuole diameter in LPS treated and LPS primed nigericin treated cells at 45 min, 2 hours respectively. Number of cells analyzed per condition = 30. ANOVA and Tukey ***($p \leq 0.001$). (D) Quantification of number of vacuoles/ µm^2 cell surface area in LPS treated and LPS primed nigericin treated cells at 45 min, 2 hours respectively. Number of cells analyzed per condition = 10. ANOVA and Tukey **($p \leq 0.001$).

LPS priming induces pro-IL-1β expression in J774A.1 macrophage cells, and nigericin treatment leads to release of IL-1β. To build off of our preliminary data, we next decided to look at more specific readouts by performing Western Blot probing for pro- and

mature forms of IL-1β on the protein lysates of stimulated J774A.1 murine macrophage cells' samples (FIG. 2A). Membrane was also probed for β-actin (FIG. 2A, bottom panel), serving as the loading control for each condition. While neither form of IL-1β was detectable in our controls, LPS-treated cells produced pro-IL-1β (31 kDa), which suggests the cells were primed to upregulate pro-inflammatory cytokine expression in response to LPS (Fig. 2A). However, mature, cleaved IL-1β (17 kDa) was not detected in any of the samples by western blotting (FIG. 2A). Semi-quantitative densitometry analysis showed that the relative expression of pro-IL-1β in 2 hour nigericin treatment (fainter band) is 3.6-fold lower compared to that of 45-minute nigericin treatment (FIG. 2B). We hypothesized that the lower levels of pro-IL-1β in the 2 hour nigericin treatment could be due to pro-IL-1β getting cleaved into its mature form and being secreted out of the cells.

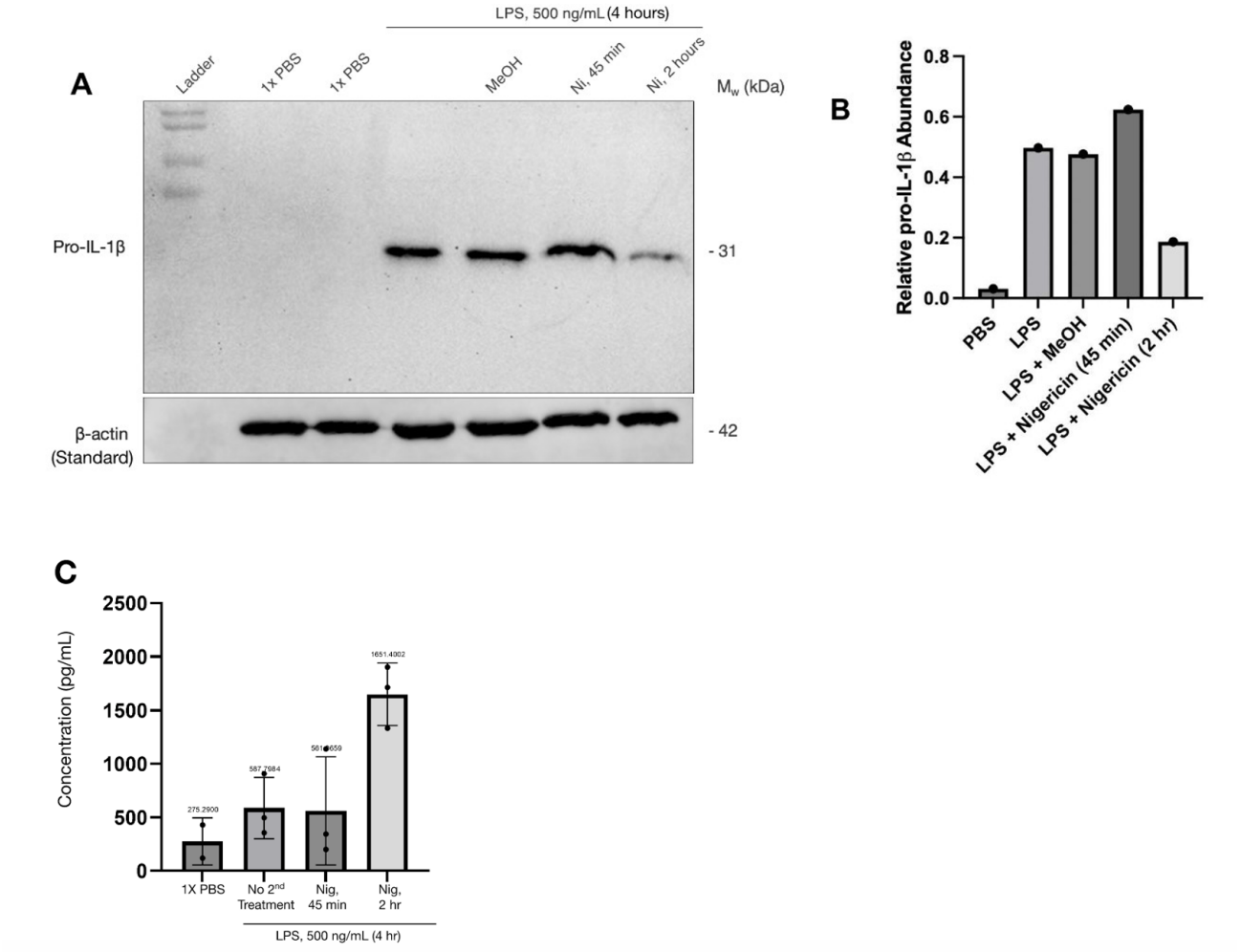

FIG. 2 Exposure of J774A.1 murine macrophage cells to LPS leads to synthesis of pro-IL- 1β and secretion of IL-1β. A) Top panel: Chemiluminescence detection after Western blot probing for pro-IL-1β (31 kDa) in protein lysates of 4 h 1 x PBS (control) and LPS-treated (500 ng/mL) J774A.1 murine macrophage cells, that have been stimulated with methanol or 10 μM nigericin for 45 minutes and 2 hours (top panel). **Bottom panel:** Chemiluminescence detection probing for β-actin (42 kDa). **B)** Densitometry analysis was performed to quantify the pixel intensity of pro-IL-1β and β-actin protein bands. The analysis was completed by taking the ratio of pro-IL-1β band density over that of the β-actin protein band in each treatment, to obtain the relative pro-IL-1β band densities. n=1. **C)** The secreted IL-1β concentrations in the experimental samples were computed using the generated standard curves from recombinant IL- 1β standards. Each bar represents the average concentration of secreted IL- 1β protein (pg/mL) at each of the indicated treatments. n = 1.

To test our hypothesis of the nigericin induced IL-1β secretion in LPS-primed mouse macrophages, we collected the supernatants of treated J774A.1 murine macrophage cells. We then quantified the secreted IL-1β protein levels in these samples using sandwich ELISA

(FIG. 2C). Even though we previously observed clear morphological indications of inflammasome activation in cells at 45-minute nigericin treatment (FIG. 1), the levels of secreted IL-1β are comparable between LPS treated macrophages (588 pg/mL) and the 45-minute nigericin treated LPS-primed macrophages (562 pg/mL) (FIG. 2C). However, the secreted IL-1β levels in the LPS-treated sample and the 45-minute nigericin treated LPS-primed sample increased by 2-fold compared to the PBS control sample (275 pg/mL) (FIG. 2C). Further, the released IL-1β level in the 2-hour nigericin treated LPS-primed macrophages (1651 pg/mL) is notably higher than that of 45-minute nigericin treated LPS-primed macrophages (562 pg/mL) (FIG. 2C). The high level of secreted IL-1β at the 2-hour nigericin treatment support that less pro-IL-1β protein is present in the lysates of 2-hour nigericin treated cells potentially because pro-IL-1β is getting cleaved into its mature form and then secreted out of the cells. However, our ELISA detects both pro- and mature forms IL-1β, so the forms of secreted IL-1β are not differentiated. To differentiate pro- and mature forms of IL-1β present in the cell culture media, we probed for pro- and mature forms of IL-1β in the protein-concentrated supernatants of each condition (Supplemental FIG. S2). Neither form of IL-1β were detected, while three non-specific bands with sizes greater than 40 kDa are observed (Supplemental FIG. S2).

Altogether, Western blot data analysis signifies that LPS (500 ng/mL) induces pro-IL-1β upregulation in J774A.1 macrophage cell model, indicating a functional priming signal in NLRP3 inflammasomes. However, since mature IL-1β was not detected after nigericin stimulation, not much can yet be concluded on NLRP3 inflammasome activation state. Further, the ELISA data suggests that LPS priming followed by nigericin stimulation results in an increased amount of both pro-IL-1β and mature IL-1β in mouse macrophages. It should be noted that our methods for detecting IL-1β in extracellular space also cannot discern whether it is being secreted by the macrophage or released by some other mechanism. Additionally, performing Western blot for the supernatants of J774A.1 murine macrophage cells treated with LPS and then stimulated with 10 μM nigericin for 45 minutes and 2 hours, is not sufficient for detecting either pro- or cleaved forms of IL-1β (Supplemental FIG. S2).

Nigericin induces cell death in LPS-primed macrophages. Despite being unable to confirm whether cleaved IL-1β was being secreted in response to nigericin, our ELISA data does indeed demonstrate that IL-1β is being released (Fig 2C). As such, we sought to glean more insight towards the kinetics of IL-1β secretion through measuring the degree of cell death between conditions using NucGreen Dead 488 staining. Differentiating between cleaved and pro-IL-1β in our cell culture supernatant is important, because the detection of IL-1β extracellular space can be attributed to not only secretion, but also cell lysis. In the former case, only mature IL-1β should be present outside of the cell, while in the latter the release of cell contents is less controlled.

The NucGreen Dead 488 reagent is a high-affinity DNA stain that stains cells with compromised cell membrane integrity (i.e., dead cells), while being unable to enter healthy cells with intact membrane. Hence, NucGreen Dead 488 stain is extremely useful for measuring viability and estimating live/dead cell ratios in a given condition. NucGreen Dead 488 then fluoresces bright green when bound to DNA, making it an effective real-time measure of cell death.

Prior to staining with NucGreen Dead 488, J774A.1 macrophages were treated with LPS (500 ng/ml) or 1x PBS (as a control) for 4 hours, and then stimulated with methanol (as a control) or 10 μM nigericin for either 45 minutes or 2 hours. Dead cells, whose DNA would be stained by the reagent due to weakened cell membrane integrity, were then imaged by fluorescence microscope (FIG. 3A). Further, the percentage of dead cells to total cell count was measured (FIG. 3B). A very low percentage of cells (around 5%) in PBS control conditions have been stained with membrane-impermeable nuclear dye, indicating minimal cell death (FIG. 3). The percentage of stained cells in LPS treatment (11%) is 2-folds greater than the PBS treatments (5%), implying that following 4 hours of LPS exposure, macrophages begin to die more quickly relative to our controls (FIG. 3). Additionally, the highest percentage of stained cells are observed in nigericin stimulated LPS-primed macrophages, with the greatest frequency of dead cells seen in the 2-hour condition (17.5%) and slightly lower dead cell percentage in the 45-minute condition (13%) (FIG. 3). The increased

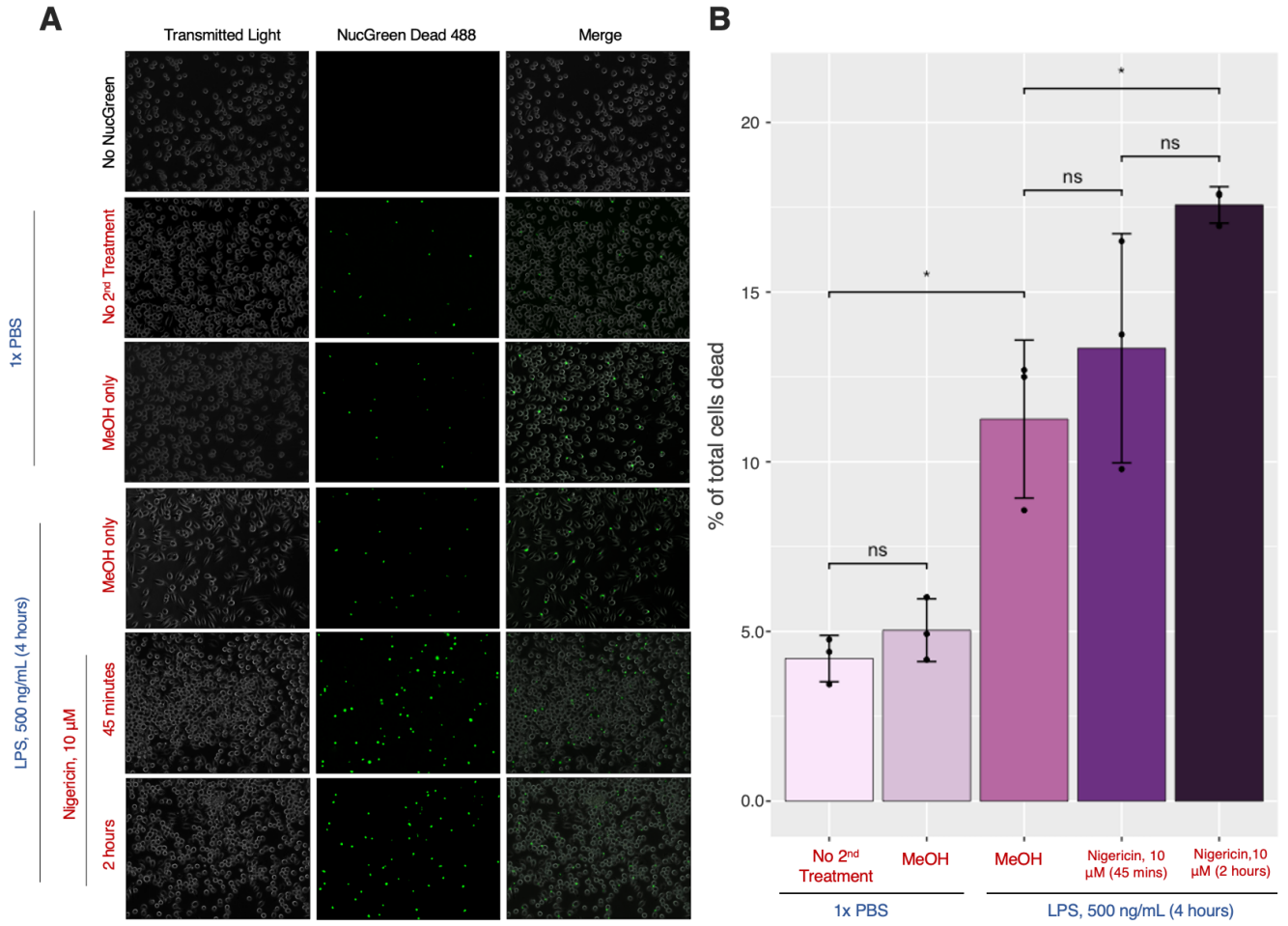

FIG. 3 Nigericin exposure induces higher rates of cell death in LPS-primed macrophages. A) (A) Representative fluorescence images (20X) of J774A.1 macrophages stained with NucGreen Dead 488. Each green dot denotes a single dead cell. (B) Percent estimate of dead cells among total cells in LPS-treated (500 ng/mL), and LPS-primed J774A.1 macrophages exposed to nigericin (10 µM) for 45 minutes or 2 hours, respectively. Oneway ANOVA with *post hoc* Tukey HSD, ns ($p > 0.05$), * ($p \leq 0.05$)

percentage of cells taking up the NucGreen Dead 488 dye following nigericin treatments suggests that nigericin promotes further cell death in murine macrophages.

LPS-primed mouse macrophages form ASC specks in response to nigericin. Our data thus far provides support that the inflammasome is plausibly activated in our mouse macrophage model given the nigericin induced irregular morphological changes and increased secreted IL-1β detected in ELISA. However, while our observed morphological changes, production of pro-IL1β and induction of cell death following nigericin exposure in LPS-primed J774A.1 macrophages are in line with the phenotypic changes expected during inflammasome activation, they are not necessarily specific downstream effects of inflammasome assembly.

To investigate the localization and aggregation of adaptor protein ASC in response to nigericin, we stained the nuclei and ASC of J774A.1 mouse macrophage cells in each condition and then observed them under an epifluorescence microscope for ASC speck localization within the cells (FIG. 4). The LPS control cells do not exhibit speck-like fluorescence signals, likely due to ASC being diffusely localized throughout the cytoplasm and nucleus of inactivated cells (14) (FIG. 4, top row). Conversely, when exposed to nigericin, we observed speck-like fluorescence signals (green) of ASC, around 1 µm in diameter, present in a perinuclear area of both 45-minute and 2-hour nigericin treated cells (FIG. 4, middle and bottom row). The frequency of speck-like fluorescence signals is higher in 2-hour nigericin treated cells compared to the 45-minute condition. Upon inflammasome

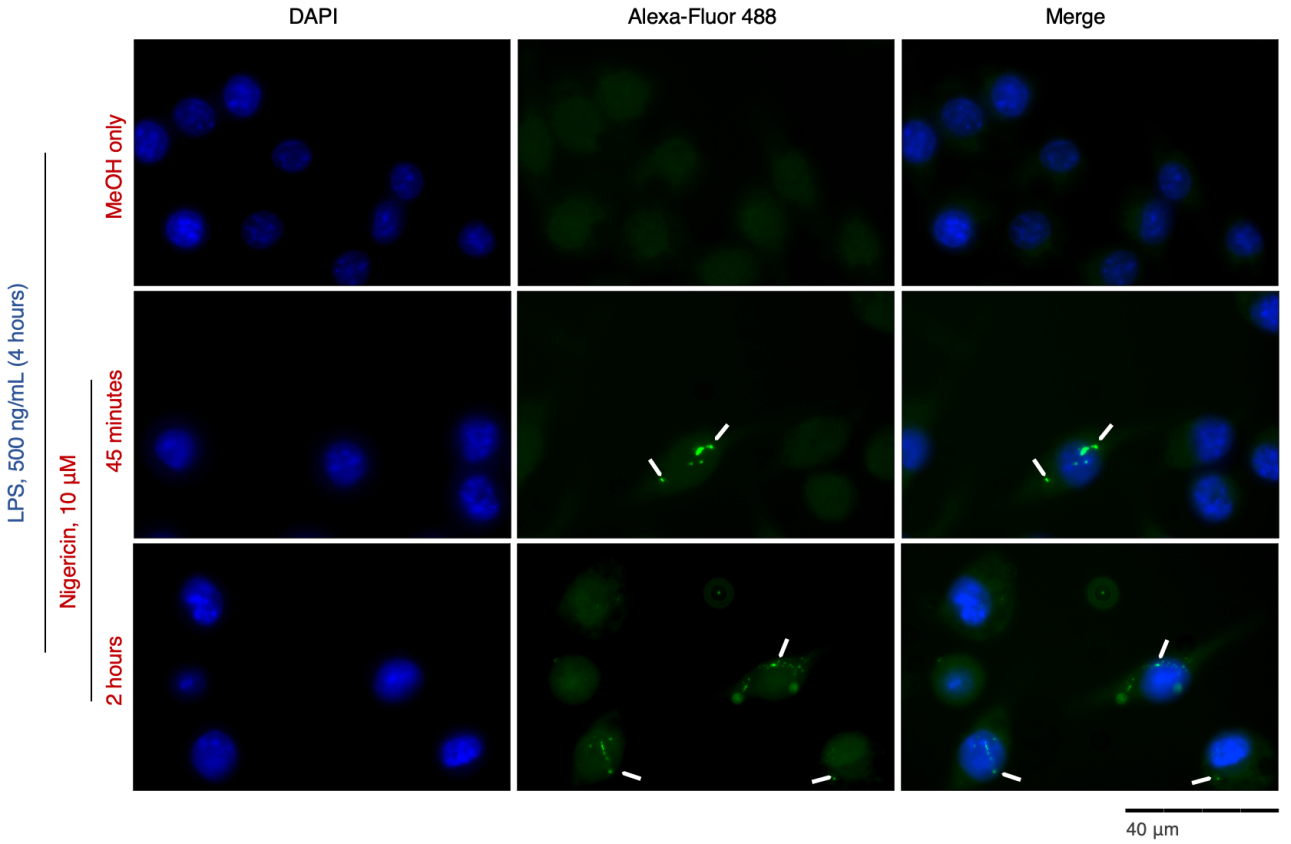

FIG. 4 LPS-primed J774A.1 murine macrophage form ASC speck aggregates in response to nigericin exposure. Immunocytochemistry of J774A.1 murine macrophages using monoclonal antibody against ASC coupled with Alexa Fluor-conjugated secondary antibody (green). Nuclear counterstain performed using DAPI (blue). Representative epi-fluorescence micrographs (100x) are shown for J774A.1 cells treated with LPS only, and LPS-primed macrophages exposed to nigericin for either 45 minutes or 2 hours. Speck-like fluorescence signals (green) of ASC (arrowheads) were observed after nigericin treatment. *Scale bar* 40 µm.

activation, the localization pattern of ASC changes from a weak diffuse signal present throughout the cell to small and localized bright specks in nigericin stimulated cells (FIG. 4). Since we observed ASC speck formation after 45 minutes of nigericin treatment, this suggests that nigericin-dependent assembly of ASC aggregates is occurring upstream of secretion of IL-1β in LPS-primed J774A.1 cells. Together our data indicate that NLR3P inflammasome activation likely occurred in our *in vitro* model.

DISCUSSION

Dysregulation in the molecular processes that govern inflammation are being found culpable in an increasing diversity of pathologies (18, 19). Given the pressing need to better understand how inflammasome activation and its downstream effects may drive or mitigate disease, it is also imperative to have well-characterized cell culture models of the inflammasome to expedite *in vitro* research. This, in turn, will support a smooth transition to studies within *in vivo* animal models and the clinic. Our study in particular, then, may be outlined by the following aims: we first established a working model in nigericin-activated murine macrophages pre-treated with LPS to induce changes in morphology associated with inflammasome activation. Afterwards, we optimized our methodologies for measuring cleaved IL-1β as a readout for inflammasome activation and developed a protocol to visually confirm inflammasome activation through visualizing ASC speck formation.

Our study contributes valuable results towards continued efforts to improve an *in vitro* mouse inflammasome model, but also leaves a number of outstanding questions that may pave the way to future studies. Among our results, the detection of ASC specks is our most compelling support that the NLRP3 inflammasome is indeed being activated within our

mouse macrophage model. Confirmation of ASC speck formation, a molecular event specific to inflammasome-mediated cell responses (18–20), is able to definitively answer the question of whether our cell culture model induces inflammasome activation at all. A strong case, then, can be made that our J774A.1 macrophage model is an appropriate *in vivo* system for further study centering the inflammasome. This has historically been difficult, as past research groups relied more exclusively on detecting cleaved IL-1β and measures of cell death as proxies for inflammasome activation (11–13). While cell death is indeed concomitant with inflammasome activation, detecting cell death alone would not provide a specific readout of pyroptotic cell death as a result of inflammasome activation (21).

Detection of cleaved IL-1β, too, has remained one of main technical challenges and the greatest limitation in our present study. We were unable to detect cleaved IL-1β within both culture supernatant and macrophage whole cell lysate. However, we observed upregulation of pro-IL-1β following LPS-mediated macrophage activation that persists with subsequent exposure to nigericin, but the mature, cleaved form was not detectable through Western blotting.

We hypothesized that cleaved IL-1β is secreted from the macrophage, and only undetectable levels remain inside cells. Our analysis of cell culture supernatant only partially corroborates this notion; LPS-primed macrophages indeed release IL-1β in response to nigericin, but we were unable to say with certainty that the cleaved form is being secreted (FIG S2), as we can detect both pro- and cleaved IL-1β in our cell supernatant samples by ELISA (FIG 2C). One likely explanation is that protein levels secreted IL-1β are simply too low to detect by Western blotting, despite efforts to concentrate our samples beforehand (FIG S2).

While we detected IL-1β release in LPS-primed, nigericin-treated macrophages, it is worth noting that only 2 hours of nigericin exposure was sufficient to bring secreted concentrations of IL-1β above what was detected in macrophages treated with LPS alone. The concentration detected at 2 hours in our study (over 1500 pg/mL) is within range of secreted IL-1β by LPS- and nigercin-activated cells reported in the literature (approximately 500-4000 pg/mL) (14, 16, 22–24). Similarly, 45 minutes of nigericin treatment was not sufficient to detect an increase in released IL-1β relative to cells that only received a priming signal (FIG. 2C). There is no evidence that LPS alone leads to IL-1β secretion in macrophages (25), though "one-signal" IL-1β secretion has been documented in monocytes (26, 27). Whether this is an artefact, and the apparent measure of IL-1β in our LPS-only condition is a result of high background, sample contamination, or a true observation remains unclear. Due to the time and financial constraints of our study, we were unable to replicate this experiment. Although more work remains to improve our understanding of IL-1β secretion in macrophages, our present data nonetheless demonstrates that nigericin stimulation does induce IL-1β from the macrophage and is therefore an important component to our cell culture model.

The results of our study, especially ASC speck visualization in our imaging data support that our working model is effective at activating the NLRP3 inflammasome. However, a number of our observations do raise some interesting, complex questions regarding the nature of this murine macrophage model. Most of the literature surrounding the NLRP3 inflammasome refer to the initiation of pyroptotic cell death (28, 29), whose phenotypic features include cell swelling and the presence of bubble-like protrusions, or "blebs" at the surface of the plasma membrane (30, 31). In this study, LPS-primed macrophages indeed increase in cell surface area in response to nigericin, but the hallmark "blebbing" is notably absent (FIG1A & B). Notably, the use of ATP, another "second signal," by a previous research group induced the "blebs" and cell swelling that are more obviously associated with pyroptosis (13). Such a contradiction to our expectations prompts the question: are we looking at pyroptosis at all?

Pyroptosis, while being the primary form of inflammatory cell death associated with the NLRP3 inflammasome, is not the only possible outcome. An alternative form of programmed cell death, necroptosis, is also both pro-inflammatory and has a well-documented association with inflammasome activation (7, 32, 33). Importantly, our LPS-pretreated macrophages adopt morphological features more similar to necroptotic cells documented in the literature (FIG. 1 A), including a more translucent cytosol (34) and vacuolization of cell components,

such as the endoplasmic reticulum and Golgi apparatus (35). Nigericin in particular has been implicated in driving necroptosis in human monocytes (36).

The possibility that nigericin-induced NLRP3 inflammasome activation is driving necroptotic, rather than pyroptotic cell death carries some intriguing implications: other "readouts" for NLRP3 inflammasome activation in this model, such as GSDMD or caspase-1, may produce negative results. While this would allow us to rule out pyroptosis, it would be necessary to use alternative assays to make full use of this cell culture model by instead probing for markers involved necroptotic cell death in this J774A.1 cell culture model. The expression of signalling molecules that induce both NLRP3 inflammasome activation and pro-necroptotic pathways, including receptor-interacting protein kinase-3 (RIPK3) (22), mixed-lineage kinase domain-like protein (MLKL) (22), and caspase-8 (37) would be appropriate parameters to measure. Given our limited data, such a presumption is still conjecture; the door is open for future research groups to explore these possibilities.

Future Directions As mentioned in the discussion, future studies may be to determine whether ASC inflammasome activation in this murine macrophage model is accompanied by either pyroptosis or necroptosis, or even compare differential inflammatory responses of known "second signals" for NLRP3 inflammasome activation to nigericin, such as ATP, cholesterol or uric acid crystals. Future research groups should also continue work towards optimizing IL-1β quantification methods and characterize the mechanisms underlying IL-1β secretion itself through the inhibition of secretory machinery (for example, microtubule formation or exosome release) (38) or inhibition or GSDMD pore formation using drugs such as disulfiram (39).

ACKNOWLEDGEMENTS

We would like to extend our gratitude towards the UBC Department of Microbiology & Immunology for funding this project, alongside Dr. Marcia Graves and Dr. Mihai Cirstea for their guidance and technical assistance throughout the term, as well as Jade Muileboom for her support as lab manager/technician. The J774A.1 macrophage cell line used in this article was a kind gift from team 2-delta (Taylor Bootsma, Brandon Connor, Yugyoung Song, and Claudia Szlavy). Lastly, we thank both teams 2-delta and 2-gamma for their camaraderie, generosity and troubleshooting advice.

CONTRIBUTIONS

All authors collaborated to prepare this manuscript. S.M. and I.Z. were responsible for results, data interpretation and writing the methods section. I.Z. and B.Y wrote the future directions. B.Y. was responsible for micrograph pseudo-colouring and cell morphology quantification, statistical analyses, figure preparation, and wrote the discussion section. S.M. also assisted with statistical analyses and figure preparation. M.J. contributed to writing the summary and introduction. All authors contributed equally laboratory time over the course of the term. All authors invested an average of 25-30 hours per week on-site at the UBC Microbiology and Immunology laboratories.

REFERENCES

1. Kelley, N., D. Jeltema, Y. Duan, and Y. He. 2019. The NLRP3 Inflammasome: An Overview of Mechanisms of Activation and Regulation. *Int J Mol Sci* 20: 3328.
2. Takeuchi, O., and S. Akira. 2010. Pattern Recognition Receptors and Inflammation. *Cell* 140: 805–820.
3. Franchi, L., T. Eigenbrod, R. Muñoz-Planillo, and G. Nuñez. 2009. The Inflammasome: A Caspase-1 Activation Platform Regulating Immune Responses and Disease Pathogenesis. *Nat Immunol* 10: 241.
4. Guo, H., J. B. Callaway, and J. P.-Y. Ting. 2015. Inflammasomes: mechanism of action, role in disease, and therapeutics. *Nat Med* 21: 677–687.
5. Nakagawa, K., E. Gonzalez-Roca, A. Souto, T. Kawai, H. Umebayashi, J. M. Campistol, J. Cañellas, S. Takei, N. Kobayashi, J. L. Callejas-Rubio, N. Ortego-Centeno, E. Ruiz-Ortiz, F. Rius, J. Anton, E. Iglesias, S. Jimenez-Treviño, C. Vargas, J. Fernandez-Martin, I. Calvo, J. Hernández-Rodríguez, M. Mendez, M. T. Dordal, M. Basagaña, S. Bujan, M. Yashiro, T. Kubota, R. Koike, N. Akuta, K. Shimoyama, N. Iwata, M. K. Saito, O. Ohara, N. Kambe, T. Yasumi, K. Izawa, T. Kawai, T. Heike, J. Yagüe, R. Nishikomori, and J. I. Aróstegui. 2015. Somatic NLRP3 mosaicism in Muckle-Wells

syndrome. A genetic mechanism shared by different phenotypes of cryopyrin-associated periodic syndromes. *Annals of the Rheumatic Diseases* 74: 603–610.
6. Booshehri, L. M., and H. M. Hoffman. 2019. CAPS and NLRP3. *J Clin Immunol* 39: 277–286.
7. Bauernfeind, F. G., G. Horvath, A. Stutz, E. S. Alnemri, K. MacDonald, D. Speert, T. Fernandes-Alnemri, J. Wu, B. G. Monks, K. A. Fitzgerald, V. Hornung, and E. Latz. 2009. Cutting Edge: NF-κB Activating Pattern Recognition and Cytokine Receptors License NLRP3 Inflammasome Activation by Regulating NLRP3 Expression1. *The Journal of Immunology* 183: 787–791.
8. Muñoz-Planillo, R., P. Kuffa, G. Martínez-Colón, B. L. Smith, T. M. Rajendiran, and G. Núñez. 2013. K+ efflux is the Common Trigger of NLRP3 inflammasome Activation by Bacterial Toxins and Particulate Matter. *Immunity* 38: 1142–1153.
9. Eigenbrod, T., and A. H. Dalpke. 2015. Bacterial RNA: An Underestimated Stimulus for Innate Immune Responses. *The Journal of Immunology* 195: 411–418.
10. Mariathasan, S., D. S. Weiss, K. Newton, J. McBride, K. O'Rourke, M. Roose-Girma, W. P. Lee, Y. Weinrauch, D. M. Monack, and V. M. Dixit. 2006. Cryopyrin activates the inflammasome in response to toxins and ATP. *Nature* 440: 228–232.
11. Dana, H. M., A. Rosen, and P. Tabassi. 2022. Towards optimizing ATP-induced activation of the NLRP3 inflammasome in glycolysis-inhibited J774A.1 murine macrophages. *Undergraduate Journal of Experimental Microbiology and Immunology* 27.
12. Sekhon, P., R. Singh, and A. Song. 2022. Investigating the role of calcium ion mobilization in NLRP3 inflammasome activation of J774A.1 macrophages and optimizing cell morphology and IL-1β quantification protocols. *Undergraduate Journal of Experimental Microbiology and Immunology* 27.
13. Cortez, S. N., J. Y. He, and V. M. Lising. 2022. Establishing a J774A.1 Murine Macrophage NLRP3 Inflammasome Model for Examining Short-Chain Fatty Acid Suppression. *Undergraduate Journal of Experimental Microbiology and Immunology* 27.
14. Nagar, A., T. Rahman, and J. A. Harton. 2021. The ASC Speck and NLRP3 Inflammasome Function Are Spatially and Temporally Distinct. *Front Immunol* 12: 752482.
15. Franklin, B. S., L. Bossaller, D. De Nardo, J. M. Ratter, A. Stutz, G. Engels, C. Brenker, M. Nordhoff, S. R. Mirandola, A. Al-Amoudi, M. S. Mangan, S. Zimmer, B. G. Monks, M. Fricke, R. E. Schmidt, T. Espevik, B. Jones, A. G. Jarnicki, P. M. Hansbro, P. Busto, A. Marshak-Rothstein, S. Hornemann, A. Aguzzi, W. Kastenmüller, and E. Latz. 2014. The adaptor ASC has extracellular and "prionoid" activities that propagate inflammation. *Nat Immunol* 15: 727–737.
16. Dick, M. S., L. Sborgi, S. Rühl, S. Hiller, and P. Broz. 2016. ASC filament formation serves as a signal amplification mechanism for inflammasomes. *Nat Commun* 7: 11929.
17. McWhorter, F. Y., T. Wang, P. Nguyen, T. Chung, and W. F. Liu. 2013. Modulation of macrophage phenotype by cell shape. *Proceedings of the National Academy of Sciences* 110: 17253–17258.
18. Strowig, T., J. Henao-Mejia, E. Elinav, and R. Flavell. 2012. Inflammasomes in health and disease. *Nature* 481: 278–286.
19. Li, Y., H. Huang, B. Liu, Y. Zhang, X. Pan, X.-Y. Yu, Z. Shen, and Y.-H. Song. 2021. Inflammasomes as therapeutic targets in human diseases. *Sig Transduct Target Ther* 6: 1–14.
20. Stutz, A., G. L. Horvath, B. G. Monks, and E. Latz. 2013. ASC Speck Formation as a Readout for Inflammasome Activation. In *The Inflammasome: Methods and Protocols*. Methods in Molecular Biology C. M. De Nardo, and E. Latz, eds. Humana Press, Totowa, NJ. 91–101.
21. Tsuchiya, K. 2020. Inflammasome-associated cell death: Pyroptosis, apoptosis, and physiological implications. *Microbiology and Immunology* 64: 252–269.
22. Conos, S. A., K. W. Chen, D. De Nardo, H. Hara, L. Whitehead, G. Núñez, S. L. Masters, J. M. Murphy, K. Schroder, D. L. Vaux, K. E. Lawlor, L. M. Lindqvist, and J. E. Vince. 2017. Active MLKL triggers the NLRP3 inflammasome in a cell-intrinsic manner. *Proceedings of the National Academy of Sciences* 114: E961–E969.
23. Mouasni, S., V. Gonzalez, A. Schmitt, E. Bennana, F. Guillonneau, S. Mistou, J. Avouac, H. K. Ea, V. Devauchelle, J.-E. Gottenberg, G. Chiocchia, and L. Tourneur. 2019. The classical NLRP3 inflammasome controls FADD unconventional secretion through microvesicle shedding. *Cell Death Dis* 10: 1–18.
24. Moretti, J., B. Jia, Z. Hutchins, S. Roy, H. Yip, J. Wu, M. Shan, S. R. Jaffrey, J. Coers, and J. M. Blander. 2022. Caspase-11 interaction with NLRP3 potentiates the noncanonical activation of the NLRP3 inflammasome. *Nat Immunol* 23: 705–717.
25. Lopez-Castejon, G., and D. Brough. 2011. Understanding the mechanism of IL-1β secretion. *Cytokine Growth Factor Rev* 22: 189–195.
26. Netea, M. G., C. A. Nold-Petry, M. F. Nold, L. A. B. Joosten, B. Opitz, J. H. M. van der Meer, F. L. van de Veerdonk, G. Ferwerda, B. Heinhuis, I. Devesa, C. J. Funk, R. J. Mason, B. J. Kullberg, A. Rubartelli, J. W. M. van der Meer, and C. A. Dinarello. 2009. Differential requirement for the activation of the inflammasome for processing and release of IL-1β in monocytes and macrophages. *Blood* 113: 2324–2335.
27. Gritsenko, A., S. Yu, F. Martin-Sanchez, I. Diaz-del-Olmo, E.-M. Nichols, D. M. Davis, D. Brough, and G. Lopez-Castejon. 2020. Priming Is Dispensable for NLRP3 Inflammasome Activation in Human Monocytes In Vitro. *Frontiers in Immunology* 11.
28. Swanson, K. V., M. Deng, and J. P.-Y. Ting. 2019. The NLRP3 inflammasome: molecular activation and regulation to therapeutics. *Nat Rev Immunol* 19: 477–489.
29. DiPeso, L., D. X. Ji, R. E. Vance, and J. V. Price. 2017. Cell death and cell lysis are separable events during pyroptosis. *Cell Death Discov.* 3: 1–10.

30. Fink, S. L., and B. T. Cookson. 2006. Caspase-1-dependent pore formation during pyroptosis leads to osmotic lysis of infected host macrophages. *Cellular Microbiology* 8: 1812–1825.
31. Yu, P., X. Zhang, N. Liu, L. Tang, C. Peng, and X. Chen. 2021. Pyroptosis: mechanisms and diseases. *Sig Transduct Target Ther* 6: 1–21.
32. Willingham, S. B., D. T. Bergstralh, W. O'Connor, A. C. Morrison, D. J. Taxman, J. A. Duncan, S. Barnoy, M. M. Venkatesan, R. A. Flavell, M. Deshmukh, H. M. Hoffman, and J. P.-Y. Ting. 2007. Microbial Pathogen-Induced Necrotic Cell Death Mediated by the Inflammasome Components CIAS1/Cryopyrin/NLRP3 and ASC. *Cell Host & Microbe* 2: 147–159.
33. Iyer, S. S., W. P. Pulskens, J. J. Sadler, L. M. Butter, G. J. Teske, T. K. Ulland, S. C. Eisenbarth, S. Florquin, R. A. Flavell, J. C. Leemans, and F. S. Sutterwala. 2009. Necrotic cells trigger a sterile inflammatory response through the Nlrp3 inflammasome. *Proceedings of the National Academy of Sciences* 106: 20388–20393.
34. Degterev, A., Z. Huang, M. Boyce, Y. Li, P. Jagtap, N. Mizushima, G. D. Cuny, T. J. Mitchison, M. A. Moskowitz, and J. Yuan. 2005. Chemical inhibitor of nonapoptotic cell death with therapeutic potential for ischemic brain injury. *Nat Chem Biol* 1: 112–119.
35. Shubin, A. V., I. V. Demidyuk, A. A. Komissarov, L. M. Rafieva, and S. V. Kostrov. 2016. Cytoplasmic vacuolization in cell death and survival. *Oncotarget* 7: 55863–55889.
36. Hentze, H., X. Y. Lin, M. S. K. Choi, and A. G. Porter. 2003. Critical role for cathepsin B in mediating caspase-1-dependent interleukin-18 maturation and caspase-1-independent necrosis triggered by the microbial toxin nigericin. *Cell Death Differ* 10: 956–968.
37. Kang, C.-W., A. Dutta, L.-Y. Chang, J. Mahalingam, Y.-C. Lin, J.-M. Chiang, C.-Y. Hsu, C.-T. Huang, W.-T. Su, Y.-Y. Chu, and C.-Y. Lin. 2015. Apoptosis of tumor infiltrating effector TIM-3+CD8+ T cells in colon cancer. *Sci Rep* 5: 15659.
38. Carta, S., S. Tassi, C. Semino, G. Fossati, P. Mascagni, C. A. Dinarello, and A. Rubartelli. 2006. Histone deacetylase inhibitors prevent exocytosis of interleukin-1β-containing secretory lysosomes: role of microtubules. *Blood* 108: 1618–1626.
39. Hu, J. J., X. Liu, S. Xia, Z. Zhang, Y. Zhang, J. Zhao, J. Ruan, X. Luo, X. Lou, Y. Bai, J. Wang, L. R. Hollingsworth, V. G. Magupalli, L. Zhao, H. R. Luo, J. Kim, J. Lieberman, and H. Wu. 2020. FDA-approved disulfiram inhibits pyroptosis by blocking gasdermin D pore formation. *Nat Immunol* 21: 736–745.